Direct-path based fingerprint extraction algorithm for indoor localization

Dali Zhu*
School of Cyber Security, University of Chinese Academy of Sciences
Institute of Information Engineering, Chinese Academy of Sciences
zhudali@iie.ac.cn

Bobai Zhao†
School of Cyber Security, University of Chinese Academy of Sciences
Institute of Information Engineering, Chinese Academy of Sciences
zhaobobai@iie.ac.cn

Siye Wang
School of Cyber Security, University of Chinese Academy of Sciences
Institute of Information Engineering, Chinese Academy of Sciences
wangsiye@iie.ac.cn

Di Wu
School of Cyber Security, University of Chinese Academy of Sciences
Institute of Information Engineering, Chinese Academy of Sciences
wudi@iie.ac.cn

ABSTRACT

At present, there has been a booming interest in utilizing Channel State Information (CSI) extracted from MIMO-OFDM PHY layer to achieve precise indoor localization. Compared with Received Signal Strength Indicator (RSSI), CSI as a fine-grained feature has a better performance on expressing the spatial and temporal features of wireless signal. As a result, CSI is more sensitive to the noise interference and multi-path. In this paper, we present a direct-path based fingerprint extraction algorithm for indoor localization in noisy and multi-path indoor environment. Our proposed algorithm firstly extracts the amplitude and phase measurements of direct-path from the raw CSI, and then calculates the unique fingerprint feature according to the filtered CSI. The experimental results show that our proposed algorithm improves the positioning accuracy up to 23.5% in complex indoor multi-path environment.

CCS CONCEPTS

• **Networks → Location based services**;

KEYWORDS

Indoor Localization, Channel State Information, Fingerprint Extraction

ACM Reference Format:
Dali Zhu, Bobai Zhao, Siye Wang, and Di Wu. 2018. Direct-path based fingerprint extraction algorithm for indoor localization. In *EAI International Conference on Mobile and Ubiquitous Systems: Computing, Networking and Services (MobiQuitous '18), November 5–7, 2018, New York, NY, USA.* ACM, New York, NY, USA, 8 pages. https://doi.org/10.1145/3286978.3286993

*Professor Zhu insisted his name be first.
†This author is the one who did all the really hard work.

MobiQuitous '18, November 5–7, 2018, New York, NY, USA

ACM ISBN 978-1-4503-6093-7/18/11…$15.00
https://doi.org/10.1145/3286978.3286993

1 INTRODUCTION

Indoor localization as one of the most important applications in Internet of Things (IoT) has received much attention from the academic and industry sectors. At present, infrared-based [27], bluetooth-based [14], Wi-Fi-based [20, 32], RFID-based [17, 25] and some other positioning technologies have been proposed. Compared with other technologies, Wi-Fi as a ubiquitous wireless signal is more suitable for indoor localization in our daily life.

Traditional signal features used to indoor localization include: the Received Signal Strength Indicator (RSSI), Time of Arrival (ToA), Time Difference of Arrival (TDoA) and Angle of Arrival (AoA) [3, 4, 21, 25, 26, 31]. However, since the spacial and temporal fluctuations in wireless signal, RSSI as a coarse-grained feature cannot precisely express the spacial features of wireless signal. At the same time, phase shift used in AoA is sensitive to the noise interference and multi-path in indoor environment, and becomes distortion. As a result, another new signal feature who can express the spacial features of wireless signal is required.

Channel State Information (CSI) as a fine-grained feature is firstly extracted from MIMO-OFDM PHY layer in off-the-shell Intel5300 Network Interface Card (NIC) by authors in [10]. Compared with RSSI, although the CSI is still susceptible to the noise and fluctuation in time and space, fine-grained subcarrier measurements in CSI increase the possibility of extraction of Line-of-Sight (LoS) and multi-path, which help us to improve the positioning accuracy. Multiple Signal Classification (MUSIC) [22] algorithm as the most efficient method is widely used in direct-path extraction, namely LoS path extraction. However, due to the fact that Symbol Time Offset (STO) and Sampling Frequency Offset (SFO) exist in the raw CSI phase measurements, the positioning accuracy of traditional MUSIC algorithm will degrade dramatically, since STO and SFO may lead to the distortion of CSI measurements. Although authors in [8] have presented the SiFi system to eliminate the interference

of STO and SFO, they still treat the SFO as a constant on the order of minutes instead of analyzing the signal feature of SFO. As a result, in this paper, we take the advantages of SFO and STO signal features to improve the MUSIC algorithm and achieve the interference attenuation.

In order to cope with the multi-path effect in indoor environment better, some new contributions are introduced to the multi-path fingerprint extraction [11, 13, 23, 28]. Authors in [28] proposed a fingerprint extraction method called Signal-Subspace Projection (SSP). According to the spacial and temporal characteristics of multi-path, SSP extracted the fingerprint feature from spacial-temporal covariance matrix. Authors in [13] improved the previous work [15] and proposed Maximum Discrimination Projection (MDP) and Maximum Discrimination Transformation (MDT). They make a comparison between SSP, MDP and MDT to test their performance according to the Cumulative Distribution Function (CDF) of localization error. The experimental results show that fingerprints generated by MDP and MDT achieves better positioning accuracy than SSP.

In this paper, we propose a direct-path based fingerprint extraction algorithm for indoor localization, which has the following contributions:

- **A direct-path based fingerprint extraction algorithm** is proposed. Our proposed algorithm has a better performance on noise attenuation and multi-path extraction. Compared with traditional filtering algorithm, such as Kalman Filter and its extended forms, the experimental results show that our proposed algorithm improves the positioning accuracy up to 23.5%.
- We explore the MUSIC algorithm for fingerprint positioning, and take the advantages of phase sanitization and multiple linear regression to achieve the direct-path extraction and corresponding amplitude estimate, the novel algorithm is referred as **ps-MUSIC**. Compared with traditional filtering algorithm which can be only used for noise removal, our proposed algorithm distinguishes between signal subspace and noise space, and extract the direct-path phase and amplitude estimates.
- **Improved Maximum Discrimination Transformation** (IMDT) is proposed, which combines the MDT with Similarity Profile (SP) algorithm to achieve the direct-path based fingerprint extraction.

The rest of this paper is organized as follows. Section 2 introduces the theory of CSI. Section 3 presents the new fingerprint extraction algorithm. Experimental results and analysis will be discussed in Section 4. In the end, Section 5 will make a conclusion about this paper.

2 RELATED WORK

2.1 Channel State Information

In 2010, authors in [10] firstly utilized off-the-shell Intel5300 Network Interface Card (NIC) to extract the CSI measurements from MIMO-OFDM PHY layer. And each CSI depicts the amplitude and phase of a subcarrier:

$$\mathbf{H}(f) = |\mathbf{H}(f)|\, e^{jsin(\angle \mathbf{H})} \tag{1}$$

where $\mathbf{H}(f)$ represents the CSI at the subcarrier with central frequency of f, $|\mathbf{H}(f)|$ is the amplitude value at the subcarrier, and $\angle\mathbf{H}$ denotes its phase.

If we consider the multi-path effect in indoor environment, CSI measurement will become the linear superposition of multi-path components, and the linear superposition may be constructive or destructive. Equation 1 will be formulated as:

$$\mathbf{H}(f_i) = \sum_{k=1}^{K} |\mathbf{H}(f_i)|\, e^{-j2\pi\tau_k^{'} f_i} \tag{2}$$

where $\mathbf{H}(f_i)$ depicts the CSI at the i-th subcarrier, $|\mathbf{H}(f_i)|$ is the amplitude value at the subcarrier, $\tau_k^{'}$ is the Time of Arrival (ToA) of k-th path, f_i is the i-th subcarrier frequency, and K represents the number of path (including multi-path and direct-path).

Supposing that a positioning system based on Wi-Fi has been equipped with m transmitting antennas and n receiving antennas. These transceiver antennas generate $m \times n$ links. At present, the CSI of 30 subcarriers can be extracted from a data packet for each link, and generates a $m \times n \times 30$ CSI matrix for these links. Compared with RSSI, CSI will provide much more information which can be used for localization service. However, one concern is that the fine-grained CSI might also mean severer temporal fluctuations, since instead of single-valued RSSI. For instance, we set a pair of transceiver antennas and send 30 IP packets to the Access Point (AP). The CSI of subcarrier 20 and subcarrier 30 at the link are extracted from these 30 receive packets, and the amplitude and phase values of these two subcarriers are shown in Figure 1.

According to the experimental results, although the CSI depicts the spacial features of the communication link, multi-path effect and noise interference still make an impact on the parameter stability. For the same packet, CSI measurements in subcarrier 20 and 30 remain independent, these two subcarriers may exist different quantities of multi-path. For the temporal fluctuation, the CSI measurements of same subcarrier in consecutive packets are quite different from each other, which means the multi-path effect and noise interference are time-varying. As a result, how to extract the direct-path based stable fingerprints becomes the motivation in this paper.

2.2 Multiple Signal Classification (MUSIC)

MUSIC algorithm is firstly proposed by authors in [22], which is used as the solution of multiple emitter location and signal parameter estimation. Researchers employ MUSIC algorithm to achieve the separation between signal subspace and noise subspace, and reduce the signal distortion caused by noise interference. However, since there are more than one object (i.e. furniture, human) existing in the indoor environment, multi-path effect is inevitable. Researchers employ clustering algorithm in MUSIC to achieve the extraction of direct-path. Furthermore, Symbol Time Offset (STO) and Sampling Frequency Offset (SFO) in measurements can not be eliminated by MUSIC, researchers in citegong2018sifi treat the SFO as a constant on the order of minutes to reduce the impact of SFO. However, as shown in Figure 2, the SFO causes the phase to grow linearly with the subcarrier index according to the experimental results in [2]. As a result, in this paper, we take the advantages of phase sanitization to achieve the SFO attenuation.

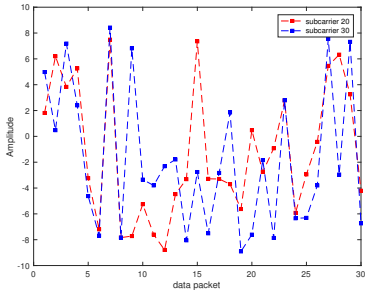

(a) Amplitude measurements in subcarrier 20 and 30

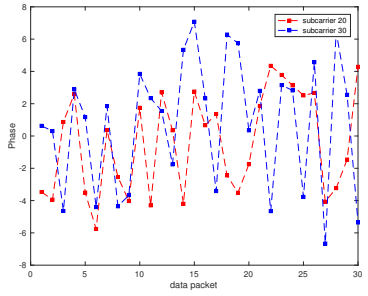

(b) Phase measurements in subcarrier 20 and 30

Figure 1: CSI measurements in subcarrier 20 and 30

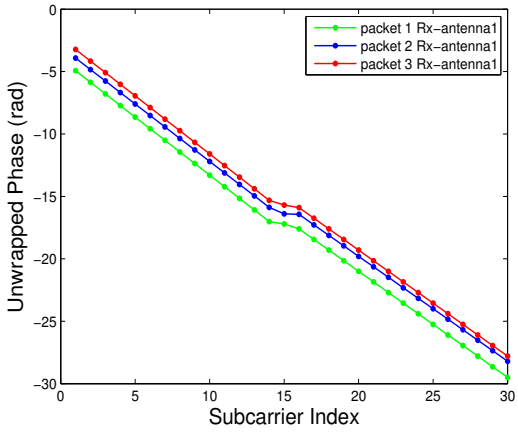

Figure 2: Unwrapped CSI phase response

2.3 Filtering algorithm

Recent years, researchers introduce machine learning, deep learning, and fuzzy set theory into fingerprint-based positioning algorithm [33]. At the same time, some traditional navigation algorithms are alsointroduced into localization service for mobile target tracking and noise removal. For instance, Kalman filter (KF) as one of the most popular state estimate techniques for linear Gaussian state-space model is widely used in spacecraft navigation and signal processing. In the aspect of noise attenuation, Kalman Filter and its extended forms (i.e. Extended Kalman Filter (EKF) and Unscented Kalman Filter (UKF)) have made contribution to the indoor localization in complex indoor environment. However, these three traditional Kalman Filter assume that the measurement noise and process noise keep constant all time, which is not appropriate in practice. Then, researchers explore the Kalman Filter, and propose Adaptive Kalman Filter. Viriational Bayes Adaptive Kalman Filter (VBAKF) is one of the most important algorithms in adaptive Kalman Filter. Although the VBAKF resolves the problem of time-varying noise, multi-path extraction cannot be inferred from Filtering algorithm. As a result, we introduce MUSIC algorithm, and make an improvement by employing phase sanitization, clustering and multiple linear regression to achieve noise attenuation, direct-path extraction and amplitude estimate. In section 4, we will make a comparison with filtering algorithm, and analyze the positioning accuracy.

2.4 Fingerprint matching algorithm

At present, the algorithms used for indoor fingerprint localization can be divided into several categories: the pattern matching algorithm, the machine learning algorithm, the neural network algorithm and so on [1, 7, 24]. The pattern matching algorithm, whose outstanding representative are K-Nearest Neighbor (KNN) and Weighted K-nearest Neighbor (WKNN), are used in the early stage and are always efficient at selecting the calibration points that are closest to the target. Since the number of nearest neighbors plays less important role in the target position estimate, the improvement effect of the former algorithms on the positioning accuracy is rather limited [5]. More and more researchers attempt to redefine the weight calculation of the calibration point [6, 9, 12]. The neural network algorithm, such as Extreme Learning Machine (ELM) is to determine the mapping path between input and output through training on the existing data set [5]. And a new input will be mapped into the most possible target location based on the neural network graph [5]. The machine learning algorithm, such as Kernel-based Ridge Regression (KRR) is to mine the useful relationship information between entities from a large amount of raw data, and establish a connection network in off-line calibration stage [18, 19]. According to the connection network, a new measurement will be assigned to the corresponding classification or transmitted into a predicted position by logistic regression. In this paper, we utilize WKNN as fingerprint matching algorithm to complete the mapping from direct-path based fingerprint to estimated coordinate.

3 DIRECT-PATH BASED FINGERPRINT EXTRACTION ALGORITHM

3.1 Phase sanitization-MUSIC

Usually, the CSI in practice always contains errors, of which the Symbol Time Offset (STO), Sampling Frequency Offset (SFO) and noise interference are major sources [8]. The STO stems from the residual error of symbol synchronization module in the receiver after the detection of frame start [8], and leads to a constant symbol offset for all symbols. According to the standard of 802.11n, the requirement of symbol synchronization is one sample resolution.

To put this in context, as the subcarrier spacing is 312.5 KHz in WiFi, a useful symbol time is 3.2 μs (excluding long/short guard interval).

As a result, the phase measurements of i-th subcarrier index, ϕ_i can be formulated as:

$$\begin{aligned} \tau_i^{'} &= \tau_i + \tau_{STO} + \tau_{i_{SFO}} + \tau_n \\ \phi_i^{'} &= \phi_i + \phi_{STO} + \phi_{i_{SFO}} + \phi_n \\ \phi_{i_{SFO}} &= -2\pi \frac{i}{N} \delta \end{aligned} \tag{3}$$

where $\phi_i^{'}$ and $\tau_i^{'}$ are the tangled phase and delay time of i-th subcarrier index in practice, respectively. ϕ_i and τ_i are the true phase and delay time of i-th subcarrier index in theory. N is the FFT size (which is 64 in IEEE 802.11n), and ϕ_n and τ_n are the added phase shift and delay time caused by noise interference.

According to the experimental results in [2], the SFO causes the phase to grow linearly with the subcarrier index. As a result, we construct a linear term $ai + b$ to mitigate SFO and STO. The linear term is formulated as:

$$\begin{aligned} a &= \frac{\phi_n^{'} - \phi_1^{'}}{i_n - i_1} = \frac{\phi_n - \phi_1}{i_n - i_1} - \frac{2\pi}{N}\delta \\ b &= \frac{1}{p}\sum_{j=1}^{p} \phi_j^{'} = \frac{1}{p}\sum_{j=1}^{p} \phi_j - \frac{2\pi\delta}{pN}\sum_{j=1}^{p} i_j + \phi_n \end{aligned} \tag{4}$$

where p is the number of subcarriers. Since the subcarrier frequencies are asymmetric, the term $\sum_{j=1}^{p} i_j \neq 0$ in equation (4). But the authors in [29] have reported that by setting this term to zero, the randomness in raw phases of 802.11n devices can be mitigated to some extent. Employing $\phi_i^{'} - (ai + b)$ to our proposed algorithm, the SFO and STO is mitigated.

Before we generate the final fingerprint data, phase and amplitude value of direct-path should be separated from the calibrated raw CSI measurements. Firstly, we will collect the CSI measurements from receiving antennas of an Access Point (AP) when the target is sending out packets. Then, we apply the MUSIC algorithm to achieve the separation between signal subspace and noise subspace, and resolve time delays of all paths. Thirdly, we utilize clustering algorithm to identify the direct path, and calculate the direct-path phase value at the same time. In the end, multiple linear regression is applied to achieve the estimate of direct-path amplitude value.

Based on Equation 2, ideally the CSI of 30 equally spaced subcarriers (f_1,f_2,...,f_{30}) in a communication link with K paths can be written in vector form as:

$$\begin{aligned} \boldsymbol{H} &= \boldsymbol{S}\boldsymbol{\alpha} \\ \boldsymbol{S} &= [\boldsymbol{s}(\tau_1), \boldsymbol{s}(\tau_2), ..., \boldsymbol{s}(\tau_K)] \\ \boldsymbol{s}(\tau) &= [e^{-j2\pi\tau f_1}, e^{-j2\pi\tau f_2}, ..., e^{-j2\pi\tau f_{30}}]^T \\ \boldsymbol{\alpha} &= [\alpha_1, \alpha_2, ..., \alpha_K]^T \\ \boldsymbol{H} &= [|H(f_1)|, |H(f_2)|, ..., |H(f_{30})|]^T \end{aligned} \tag{5}$$

where the size of channel matrix $\boldsymbol{H}$ is 30×1, the steering matrix $\boldsymbol{S}$ is of size $30 \times K$, the amplitude matrix $\boldsymbol{\alpha}$ is of size $K \times 1$, $\boldsymbol{s}(\tau_k)$ as the steering vector is of size 30×1. In this paper, we use $H(f_i)$ to denote $|H(f_i)|$ for brevity

According to the reference in [30], we observe that the number of available subcarriers is much larger than the number of paths. For instance, with Intel5300 NIC, the CSI is of length 30 for an antenna in a packet, whereas the number of dominant paths for indoor environments is around 5. As a result, we form a Hankel matrix instead of covariance matrix for $\boldsymbol{H}$ as follows:

$$\mathbb{H} = Hankel(H) = \begin{bmatrix} H(f_1) & H(f_2) & \cdots & H(f_{30-l}) \\ H(f_2) & H(f_3) & \cdots & H(f_{30-l+1}) \\ \vdots & \vdots & \vdots & \vdots \\ H(f_{l+1}) & H(f_{l+2}) & \cdots & H(f_{30}) \end{bmatrix} \tag{6}$$

where l is an integer parameter that satisfies $l \geq K$ and $30 - l \geq K$. In this paper, we set $l = 10$. Actually, Hankel matrix proposed in 1795 is widely used in the super-resolution algorithms [16]. Then, we apply singular value decomposition on $\mathbb{H}$, i.e.

$$\mathbb{H} = \boldsymbol{U}\Sigma\boldsymbol{V}^* \tag{7}$$

where the unitary matrix $\boldsymbol{U}$ is size of $l \times l$, Σ is an $l \times (30-l)$ diagonal matrix, $\boldsymbol{V}^*$ is an $(30-l) \times (30-l)$ unitary matrix, and $*$ denotes conjugate transpose. In this paper, unitary matrix $\boldsymbol{U}$ and diagonal matrix Σ are our research emphasis. In particular, the diagonal elements $(\beta_1, \beta_2, ..., \beta_K, 0, ..., 0)$ in Σ represent the singular values $\beta_1 \geq \beta_2 \geq ... \geq \beta_K > 0$. Based on these singular values, $\boldsymbol{U}$ can be divided into two subspaces: the signal subspace whose size is $l \times K$, referred as $\boldsymbol{U}_s$, and $l \times (l-K)$ noise subspace, referred as $\boldsymbol{U}_n$. These two subspaces are corresponding to the non-zero singular values and diagonal elements of zero in Σ, respectively.

Until now, our derivation has a common assumption, namely K as a priori knowledge is known to us. However, since there may exist different K values for different packets, we need a flexible estimation method for K value. In this paper, we introduce the singular value-based threshold method according to the SiFi system [8]. In the theoretical conditions, the number of K positive singular values in Σ keeps constant. But with the noise interference, the diagonal zero elements in Σ may become positive, and leading to the more singular values than expected. For instance, Figure 2 shows the diagonal values in Σ. Since the noise interference in indoor environment, the diagonal elements of Σ all become positive, which disturb the separation between signal and noise subspace. In singular value-based threshold method, we set a threshold γ to estimate K. In particular, the singular value who is no less than $\gamma\beta_{min}$ is considered effective in signal subspace. β_{min} is the minimal singular value. According to the experimental results in [8], we set $\gamma = 8$ for moderate SNR scenarios, and $\gamma = 25$ for high SNR scenarios. The green dotted line in Figure 2 depicts the threshold for moderate SNR scenarios.

Note that, the noise subspace $\boldsymbol{U}_n$ should be orthogonal to the steering matrix $\boldsymbol{S}$, where $\boldsymbol{S} = [\boldsymbol{s}(\tau_1), \boldsymbol{s}(\tau_2), ..., \boldsymbol{s}(\tau_K)]$, and $\boldsymbol{s}(\tau) = [e^{-j2\pi\tau f_1}, e^{-j2\pi\tau f_2}, ..., e^{-j2\pi\tau f_{30}}]^T$. As a result, the ToA spread (τ_1, τ_2, ..., τ_K) can be formulated as the peaks of the following orthogonal projection function:

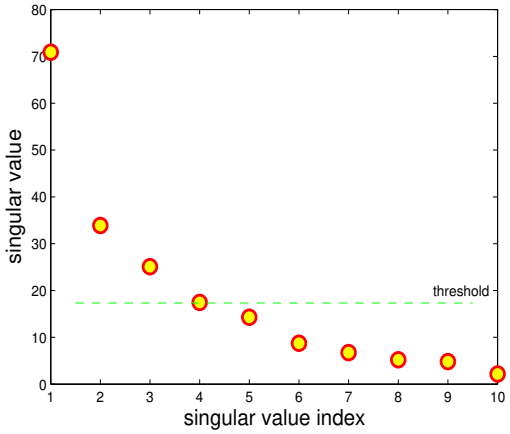

Figure 3: A sample of singular values

$$D(\tau) = \frac{1}{\|\boldsymbol{U}_n \boldsymbol{s}(\tau)\|_2} \tag{8}$$

To solve the equation above, we introduce the polynomial root finding method. Specifically, since subcarriers in the same communication link are equally spaced, we use a symbol Δf to denote the frequency spacing of two consecutive subcarriers (Δf = 321.5 kHz×4 = 1.25 MHz), and the steering vector can be rewritten as:

$$\boldsymbol{s}(\tau) = e^{-j2\pi f_{i_1}\tau}[1, z, ..., z^{l-1}]^T \tag{9}$$

$$z = e^{-j2\pi\Delta f\tau} \tag{10}$$

At the same time, $D(\tau)$ in Equation (7) can be transformed into:

$$\begin{aligned} D(\tau)^{-1} &= \boldsymbol{s}(\tau)^* \boldsymbol{C} \boldsymbol{s}(\tau) \\ \boldsymbol{C} &= \boldsymbol{U}_n \boldsymbol{U}_n^* \end{aligned} \tag{11}$$

Employing Equation (8) into (10), we can obtain:

$$D(\tau)^{-1} = e^{-j2\pi f_{i_1}\tau}\widetilde{D}(\tau)^{-1} \tag{12}$$

$$\widetilde{D}(\tau)^{-1} = \sum_{p=-l+1}^{l-1} c_p z^{-p} \tag{13}$$

$$c_p = \sum_{i-j=p} \boldsymbol{C}(i,j) \tag{14}$$

where i and j represent the row and column index of $\boldsymbol{C}$, respectively. c_p depicts the sum of elements in $\boldsymbol{C}$ along the p-th diagonal.

According to the theory of polynomial, there are $(2l-2)$ roots in Equation (12). These roots can be divided into $(l-1)$ pairs, and only $(l-1)$ roots within the unit circle carry the effective parameter τ. In these $(l-1)$ roots, we pick up the K entities who are closest to the unit circle, and employ these K values into Equation (9) to obtain the ToA spread $(\hat{\tau}_1, \hat{\tau}_2, ..., \hat{\tau}_K)$.

Now, the phase values of multi-path have been calculated, we rewrite the Equation (2) into matrix form to estimate the amplitude values of multi-path:

$$\begin{bmatrix} \hat{\alpha}_1 e^{-j2\pi f_1 \hat{\tau}_1} & \hat{\alpha}_2 e^{-j2\pi f_1 \hat{\tau}_2} & \dots & \hat{\alpha}_K e^{-j2\pi f_1 \hat{\tau}_K} \\ \hat{\alpha}_1 e^{-j2\pi f_2 \hat{\tau}_1} & \hat{\alpha}_2 e^{-j2\pi f_2 \hat{\tau}_2} & \dots & \hat{\alpha}_K e^{-j2\pi f_2 \hat{\tau}_K} \\ \vdots & \vdots & \vdots & \vdots \\ \hat{\alpha}_1 e^{-j2\pi f_{30} \hat{\tau}_1} & \hat{\alpha}_2 e^{-j2\pi f_{30} \hat{\tau}_2} & \dots & \hat{\alpha}_K e^{-j2\pi f_{30} \hat{\tau}_K} \end{bmatrix} = \begin{bmatrix} \boldsymbol{H}_1 \\ \boldsymbol{H}_2 \\ \vdots \\ \boldsymbol{H}_K \end{bmatrix} \tag{15}$$

where $(f_1, f_2, ..., f_{30})$ depicts the frequencies of 30 subcarriers, which can be calculated by the parameter Δf and Wi-Fi central frequency. According to the theory of multi linear regression, the amplitude values $(\hat{\alpha}_1, \hat{\alpha}_2, ..., \hat{\alpha}_K)$ corresponding to the K paths can be approximated successfully.

Until now, we have completed the ToA spread and amplitude value extraction of multi-path for a single data packet. In order to extract the values of direct-path, we have to conduct the procedures above on large number of data packets, and employ the Gaussian Mixture Model based clustering algorithm to achieve the classification of different paths. Then, we utilize a cascaded filter to achieve the direct-path extraction.

Firstly, the cascaded filter identify the number of different clusters. We assume that the number of direct-path cluster should be larger than 50% of the number of clustered packets. Then, the cascaded filter check the variance of different clusters, namely the variance of direct-path cluster should be less than 1.5 times sampling time. According to the 802.11n standard, one sampling time is equal to the symbol time in STO mentioned above. After the filtering operations have been finished, we obtain the direct-path cluster, and the ToA spread and amplitude values of direct-path are equal to the corresponding expectation of entities in direct-path cluster.

3.2 Diagonal Maximum Discrimination Transformation

After we extract the phase and amplitude values of direct-path, we will calculate the fingerprint vector for indoor localization. For a calibration point i, L CSI measurements extracted from L data packets is transformed into L CSI vectors by vector operation. Firstly, we calculate the channel covariance matrix at position i as:

$$\boldsymbol{R}_i = \frac{\sum_{l=1}^{L} \boldsymbol{X}_i(t_l)\boldsymbol{X}_i(t_l)^T}{\mathbf{tr}(\sum_{l=1}^{L} \boldsymbol{X}_i(t_l)\boldsymbol{X}_i(t_l)^T)} \tag{16}$$

where $\{\boldsymbol{X}_i(t_l)\}_{l=1}^{L}$ denotes the CSI vector. Employing vector operation on $\boldsymbol{R}_i$, we can obtain:

$$\boldsymbol{r}_i = \boldsymbol{vec}(\boldsymbol{R}_i^T) \tag{17}$$

Then, we calculate the matrix, which is composed of $\boldsymbol{r}_i$ ($i \in 1, 2, ..., K$) of K calibration points, referred as $\boldsymbol{R}$:

$$\boldsymbol{R} = [\boldsymbol{r}_1, \boldsymbol{r}_2, ..., \boldsymbol{r}_K] \tag{18}$$

In this paper, we introduce a normalization parameter ρ_i [13] for the projection vector:

$$\rho_i = \boldsymbol{sqrt}(\boldsymbol{r}_i^H (\boldsymbol{R}\boldsymbol{R}^H)^{-2} \boldsymbol{r}_i) \tag{19}$$

Using $\boldsymbol{R}$ and $\boldsymbol{r}_i$ to calculate the projection vector $\boldsymbol{p}_i$, and make the maximum discrimination analysis:

$$\boldsymbol{p}_i = \rho_i(\boldsymbol{R}\boldsymbol{R}^H + \beta\boldsymbol{I})^{-1}\boldsymbol{r}_i \tag{20}$$

where β is a diagonal loading parameter, which is used to reduce the fluctuation of inverted matrix caused by small eigenvalues. $\boldsymbol{I}$ is the identity matrix. According to the equatuion (19), the transformation matrix $\boldsymbol{P}_i$ is formulated as $\boldsymbol{p}_i = \boldsymbol{vec}(\boldsymbol{P}_i)$.

Employing Similarity Profile (SP) to generate the direct-path based fingerprint s_i at each calibration point i.

$$\begin{aligned} \boldsymbol{s}_i &= [s_{i1}, ..., s_{ii}, ..., s_{iK}] \\ s_{ij} &= \boldsymbol{tr}(\boldsymbol{P}_j\boldsymbol{R}_i) \end{aligned} \tag{21}$$

where s_{ij} represents the projection of covariance matrix at point i on the transformation matrix at point j. Obviously, the direct-path based fingerprint demonstrates the discrimination between different calibration points or test points. This characteristic will help the fingerprint positioning algorithm to improve the positioning accuracy.

4 EXPERIMENTAL RESULT AND ANALYSIS

4.1 Experimental setup

As shown in Figure 3, the experimental scenario is set in an empty room of $50m^2$. The ground is divided into 42 calibration points, and the distance between adjacent calibration points is $1.2m$. We set an Access Point (AP) with single antenna as signal transmitter in the center of the ground. A laptop equipped with Intel5300 NIC with three antennas as signal receiver is our positioning target. Some frothy cuboids are randomly placed in the experimental scenario as obstacles to increase the noise interference. Firstly, we collect the CSI measurements at each calibration point without obstacles to generate the calibration fingerprint. Then, in online positioning stage, we measure the CSI measurements of unknown position with obstacles and generate the online fingerprint. In the end, direct-path based fingerprint extraction algorithm and WKNN are employed to achieve the position estimate of online fingerprint in complex indoor multi-path environment.

Figure 4: Experimental scenario

4.2 Positioning accuracy

In this paper, we propose a direct-path based fingerprint extraction algorithm, which can be applied in complex indoor environment. To demonstrate the effectiveness of noise removal of our proposed algorithm, we make a comparison with Variational Bayes Adaptive Kalman Filter (VBAKF), Kalman Filter whose process noise covariance matrix (PNCM) and measurement noise covariance matrix (MNCM) are identity matrix and **diag**(100), and hard-coded noise floor of -92dBm. Figure 5 displays four real target coordinates and corresponding estimated position by these four methods. Table 1 calculates the mean positioning errors of seven target positions. According to the experimental results, when we employ IMDT and WKNN as fingerprint extraction and positioning algorithms, our proposed ps-MUSIC outperforms three other filtering algorithms in positioning accuracy. Compared with KF(1,100), VBAKF, and hard-coded noise floor, our proposed ps-MUSIC improves the positioning accuracy by 23.5%, 13.7% and 4.4%, respectively. The experimental results effectively demonstrate the effectiveness of our proposed algorithm.

Although, from the average effect point of view, our algorithm is better, but in some special positioning points, the performance of our proposed algorithm may be poor. For instance, in the positioning point (2.5, 2.5), VBAKF and Hard-coded performs better than our proposed algorithm. That is because the distance between receiver antennas and AP is Line-of-Sight (LoS), namely there is no obstacle existing when the wireless signal propagates from AP to receiver. As a result, multi-path effect will be reduced, the factor affects positioning accuracy becomes background noise. And, VBAKF as adaptive filtering algorithm, which can capture the time-varying fluctuation of measurement noise, shows the superiority of denoising.

5 CONCLUSION

In this paper, we propose a direct-path based fingerprint extraction algorithm from the perspective of multi-path effect. Our proposed algorithm takes the advantages of phase sanitization, MUSIC and multiple linear regression to infer the ps-MUSIC algorithm, and employs the improved Maximum Discrimination Transformation (IMDT) to achieve the distinguish between signal and noise subspaces, SFO and STO attenuation, direct-path and corresponding amplitude fingerprint extraction. The experimental results show that, compared with KF(1,100), VBAKF, and hard-coded noise floor, our proposed ps-MUSIC improves the positioning accuracy by 23.5%, 13.7% and 4.4%, respectively.

6 ACKNOWLEDGEMENT

This work was supported in by the National Natural Science Foundation of China (No. 61701494) and the National Key Research and Development Program of China-the Key Technologies for High Security Mobile Terminals (Grant No.2017YFB0801903).

REFERENCES

[1] Bozkurt, S., Elibol, G., Gunal, S., Yayan, U.: A comparative study on machine learning algorithms for indoor positioning. In: Innovations in Intelligent SysTems and Applications (INISTA), 2015 International Symposium on. pp. 1–8. IEEE (2015)
[2] Chowdhury, T.Z.: Using Wi-Fi channel state information (CSI) for human activity recognition and fall detection. Ph.D. thesis, University of British Columbia (2018)

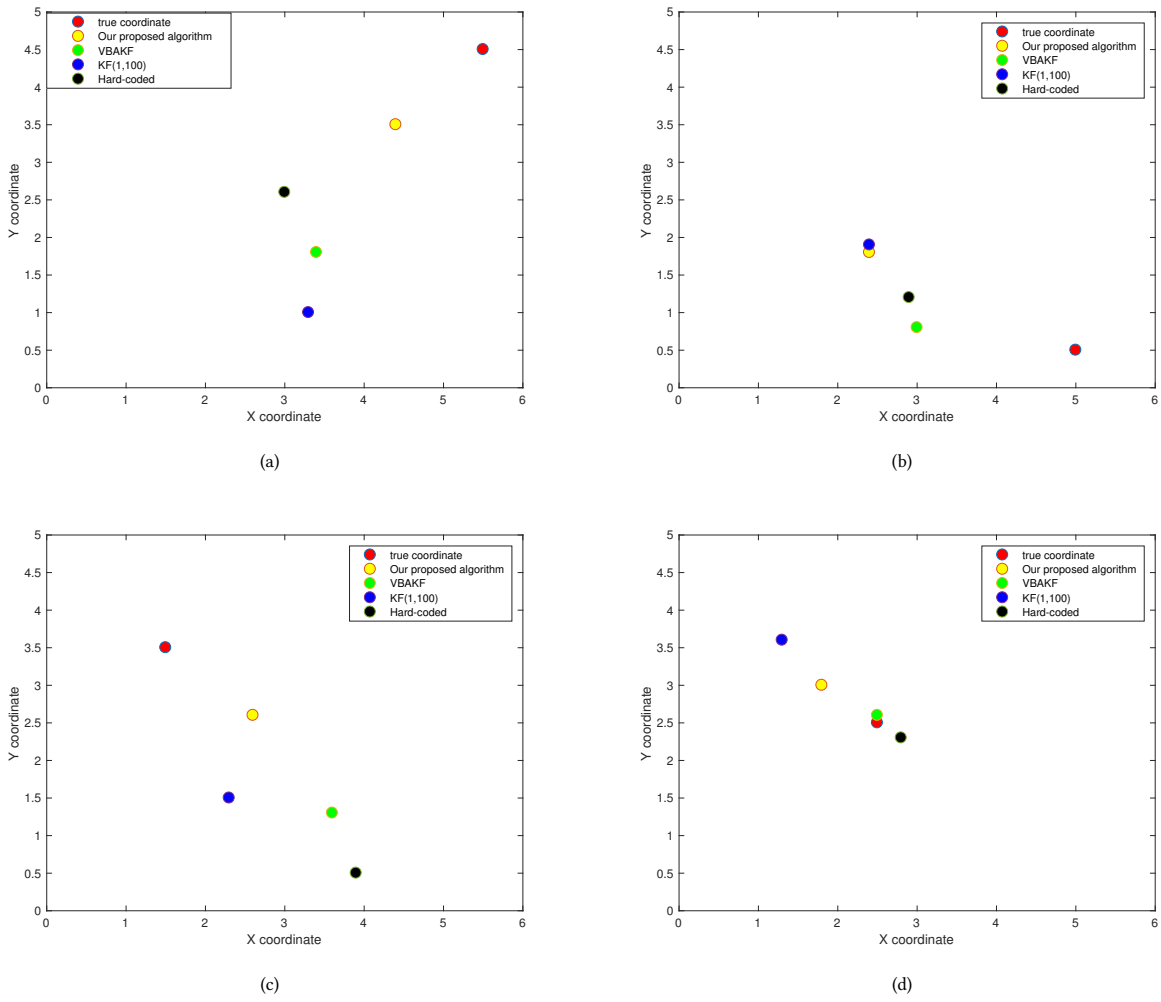

Figure 5: true coordinate and position estimates by our proposed algorithm and three filtering algorithms

Table 1: Mean positioning errors

localization error (m) / method / coordinate	Our algorithm	VBAKF	KF(1,100)	Hard-coded
(0.5,4)	2.6683	2.4413	2.7295	2.5
(1.5,3.5)	1.4213	3.0414	2.1541	3.8419
(2.5,2.5)	0.8602	0.1	1.6279	0.3606
(3,1.5)	0.9434	1.253	0.7616	0.4243
(5,0.5)	2.9069	2.0224	2.953	2.2136
(5.5,0.5)	2.6627	2.0248	3.2849	1.6401
(5.5,4.5)	1.4866	4.134	3.4205	2.571
Mean errors	1.85	2.145	2.419	1.936

[3] Cui, W., Wu, S., Wang, Y., Shan, Y.: A gossip-based tdoa distributed localization algorithm for wireless sensor networks. In: International Symposium on Instrumentation and Measurement, Sensor Network and Automation. pp. 841–846 (2014)
[4] Eickhoff, R., Ellinger, F., Mosshammer, R., Weigel, R.: 3d-accuracy improvements for tdoa based wireless local positioning systems. In: GLOBECOM Workshops. pp. 1–6 (2008)
[5] Fang, X., Nan, L., Jiang, Z., Chen, L.: Noise-aware fingerprint localization algorithm for wireless sensor network based on adaptive fingerprint kalman filter. Computer Networks **124**, 97–107 (2017)
[6] Fang, Y., Deng, Z., Xue, C., Jiao, J., Zeng, H., Zheng, R., Lu, S.: Application of an improved k nearest neighbor algorithm in wifi indoor positioning. In: China Satellite Navigation Conference (CSNC) 2015 Proceedings: Volume III. pp. 517–524. Springer (2015)
[7] Gogolak, L., Pletl, S., Kukolj, D.: Neural network-based indoor localization in wsn environments. Acta Polytechnica Hungarica **10**(6), 221–235 (2013)
[8] Gong, W., Liu, J.: Sifi: Pushing the limit of time-based wifi localization using a single commodity access point. Proceedings of the ACM on Interactive, Mobile, Wearable and Ubiquitous Technologies **2**(1), 10 (2018)
[9] Guowei, Z., Zhan, X., Dan, L.: Research and improvement on indoor localization based on rssi fingerprint database and k-nearest neighbor points. In: Communications, Circuits and Systems (ICCCAS), 2013 International Conference on. vol. 2, pp. 68–71. IEEE (2013)
[10] Halperin, D., Hu, W., Sheth, A., Wetherall, D.: Predictable 802.11 packet delivery from wireless channel measurements. In: ACM SIGCOMM 2010 Conference. pp. 159–170 (2010)
[11] Hilsenrath, O., Wax, M.: Radio transmitter location finding for wireless communication network services and management (2000)
[12] Hossain, A.M., Soh, W.S.: Cramer-rao bound analysis of localization using signal strength difference as location fingerprint. In: INFOCOM, 2010 Proceedings IEEE. pp. 1–9. IEEE (2010)
[13] Jaffe, A., Wax, M.: Single-site localization via maximum discrimination multipath fingerprinting. IEEE Transactions on Signal Processing **62**(7), 1718–1728 (2014)
[14] Jiang, D.X., Ming-Qing, H.U., Chen, Y.Q., Liu, J.F., Zhou, J.Y.: Adaptive bluetooth location method based on kernel ridge regression. Application Research of Computers **27**(9), 3487–3486 (2010)
[15] Kupershtein, E., Wax, M., Cohen, I.: Single-site emitter localization via multipath fingerprinting. IEEE Transactions on signal processing **61**(1), 10–21 (2013)
[16] Liao, W., Fannjiang, A.: Music for single-snapshot spectral estimation: Stability and super-resolution. Applied & Computational Harmonic Analysis **40**(1), 33–67 (2014)
[17] Ma, H., Wang, K.: Fusion of rss and phase shift using the kalman filter for rfid tracking. IEEE Sensors Journal **17**(11), 3551–3558 (2017)
[18] Mahfouz, S., Mourad-Chehade, F., Honeine, P., Farah, J., Snoussi, H.: Target tracking using machine learning and kalman filter in wireless sensor networks. IEEE Sensors Journal **14**(10), 3715–3725 (2014)
[19] Mahfouz, S., Mourad-Chehade, F., Honeine, P., Snoussi, H., Farah, J.: Kernel-based localization using fingerprinting in wireless sensor networks. In: Signal Processing Advances in Wireless Communications (SPAWC), 2013 IEEE 14th Workshop on. pp. 744–748. IEEE (2013)
[20] Qian, K., Wu, C., Yang, Z., Liu, Y., Jamieson, K.: Widar: Decimeter-level passive tracking via velocity monitoring with commodity wi-fi. In: The ACM International Symposium. pp. 1–10 (2017)
[21] Qian, K., Wu, C., Yang, Z., Zhou, Z., Wang, X., Liu, Y.: Enabling phased array signal processing for mobile wifi devices. IEEE Transactions on Mobile Computing **PP**(99), 1–1 (2017)
[22] Schmidt, R.O.: Multiple emitter location and signal parameter estimation. IEEE Transactions on Antennas & Propagation **34**(3), 276–280 (1986)
[23] Shata, A.M., El-Hamid, S.S.A., Heiba, Y.A., Nasr, O.A.: Multi-site fusion for wlan based indoor localization via maximum discrimination fingerprinting. In: Innovative Trends in Computer Engineering (ITCE), 2018 International Conference on. pp. 214–218. IEEE (2018)
[24] Tran, T.D., Oliveira, J., Silva, J.S., Pereira, V., Sousa, N., Raposo, D., Cardoso, F., Teixeira, C.: A scalable localization system for critical controlled wireless sensor networks. In: Ultra Modern Telecommunications and Control Systems and Workshops (ICUMT), 2014 6th International Congress on. pp. 302–309. IEEE (2014)
[25] Wang, Y., Xu, X.: Indoor localization service based on the data fusion of wi-fi and rfid. In: IEEE International Conference on Web Services. pp. 180–187 (2016)
[26] Wang, Y., Ho, K.C.: An asymptotically efficient estimator in closed-form for 3-d aoa localization using a sensor network. IEEE Transactions on Wireless Communications **14**(12), 6524–6535 (2015)
[27] Want, R., Hopper, A., Gibbons, J.: The active badge location system. ACM Transactions on Information Systems **10**(1), 91–102 (1992)
[28] Wax, M., Meng, Y., Hilsenrath, O.: Subspace signature matching for location ambiguity resolution in wireless communication systems (2000)
[29] Wu, C., Yang, Z., Zhou, Z., Qian, K., Liu, Y., Liu, M.: Phaseu: Real-time los identification with wifi. In: Computer Communications (INFOCOM), 2015 IEEE Conference on. pp. 2038–2046. IEEE (2015)
[30] Xiong, J., Jamieson, K.: Arraytrack: a fine-grained indoor location system. Usenix (2013)
[31] Xu, E., Ding, Z., Dasgupta, S.: Target tracking and mobile sensor navigation in wireless sensor networks. IEEE Transactions on Mobile Computing **12**(1), 177–186 (2012)
[32] Yang, Z., Zhou, Z., Liu, Y.: From rssi to csi: Indoor localization via channel response. ACM Computing Surveys **46**(2), 1–32 (2013)
[33] Zhu, D., Zhao, B., Wang, S.: Mobile target indoor tracking based on multi-direction weight position kalman filter. Computer Networks (2018)